
A UNIFIED MATRIX-SPECTRAL FRAMEWORK FOR STABILITY AND INTERPRETABILITY IN DEEP LEARNING

Ronald Katende

Department of Mathematics

Kabale University

Kikungiri Hill, Katuna Road, 317, Kabale, Uganda

rkatende@kab.ac.ug

ABSTRACT

We develop a unified matrix-spectral framework for analyzing stability and interpretability in deep neural networks. Representing networks as data-dependent products of linear operators reveals spectral quantities governing sensitivity to input perturbations, label noise, and training dynamics.

We introduce a Global Matrix Stability Index that aggregates spectral information from Jacobians, parameter gradients, Neural Tangent Kernel operators, and loss Hessians into a single stability scale controlling forward sensitivity, attribution robustness, and optimization conditioning. We further show that spectral entropy refines classical operator-norm bounds by capturing typical, rather than purely worst-case, sensitivity.

These quantities yield computable diagnostics and stability-oriented regularization principles. Synthetic experiments and controlled studies on MNIST, CIFAR-10, and CIFAR-100 confirm that modest spectral regularization substantially improves attribution stability even when global spectral summaries change little.

The results establish a precise connection between spectral concentration and analytic stability, providing practical guidance for robustness-aware model design and training.

Keywords analytic stability · spectral entropy · Jacobian spectra · neural tangent kernel · attribution robustness

1 Introduction

Feedforward neural networks admit the standard representation as data-dependent products of linear maps and diagonal gating operators induced by coordinate-wise nonlinearities. This follows from the chain rule and is widely used in analyses of signal propagation and stability [1]. Consequently, many analyses reduce properties of trained networks to spectra of a small number of associated operators.

Several lines of work study these operators separately. Algorithmic stability theory analyzes sensitivity of training procedures to dataset perturbations [2, 3]. Random matrix studies characterize spectral behavior of weights and end-to-end operators in high dimensions [1, 4]. Empirical work studies robustness of feature attributions under input perturbations [5]. Kernel analyses show that gradient descent dynamics are governed by Gram matrices of parameter Jacobians through the Neural Tangent Kernel [6, 7, 8]. Empirical investigations of Jacobian and Hessian spectra reveal structures related to optimization and generalization [9, 10]. These results indicate that forward sensitivity, training dynamics, curvature, and attribution stability are controlled by closely related matrix operators.

This work develops a unified analytic framework that treats these operators jointly. Rather than re-deriving known results, we organize standard constructions into a single matrix formulation and isolate spectral quantities governing stability across representations, parameters, and training dynamics.

Our main contribution is a *Global Matrix Stability Index* that aggregates spectral information from end-to-end linearizations, input Jacobians, NTK Gram matrices, and parameter Hessians. We show that these known stability properties admit a common spectral control quantity. We further introduce a spectral entropy functional capturing

typical sensitivity beyond worst-case directions. These quantities yield computable diagnostics and regularization targets linking robustness and interpretability through matrix spectra.

1.1 Related Work

Algorithmic stability, introduced in [2] and refined for stochastic gradient descent in [3], concerns robustness of training algorithms rather than analytic stability of learned predictors.

Spectral analyses of deep networks include signal propagation and random matrix approaches [1] and exact solutions for deep linear models. Empirical studies document heavy-tailed and low-rank spectral structure in trained networks [4], without analytic links to attribution robustness.

The NTK framework shows that wide-network training evolves as kernel dynamics governed by parameter Jacobian Gram matrices [6, 7, 8]. Empirical analyses further relate Jacobian and Hessian spectra to optimization and generalization behavior [10]. Our framework places these operators within a single analytic representation.

Robustness of feature attributions has been studied empirically using perturbation criteria [5]. Here attribution sensitivity is expressed directly through Jacobian perturbations, allowing analytic stability guarantees.

2 Preliminaries and Notation

We consider feedforward networks composed of linear maps and coordinate-wise nonlinearities. Let $W_i \in \mathbb{R}^{n_i \times n_{i-1}}$ denote the weight matrix of layer i and ϕ_i the activation. For inputs $x \in \mathbb{R}^{n_0}$, at points where the network is differentiable the input Jacobian admits the standard product form

$$J_f(x) = W_L D_{L-1}(x) W_{L-1} \cdots D_1(x) W_1, \quad (2.1)$$

where each $D_i(x)$ is the diagonal matrix of activation derivatives evaluated at the pre-activations of layer i [1].

Assume each activation ϕ_i is locally Lipschitz and differentiable almost everywhere, so that f is differentiable almost everywhere on \mathbb{R}^{n_0} . The input Jacobian

$$J_f(x) = \frac{\partial f(x)}{\partial x} \quad (2.2)$$

coincides almost everywhere (with respect to Lebesgue measure on \mathbb{R}^{n_0}) with the end-to-end product operator

$$\mathcal{P}(x) = W_L D_{L-1}(x) W_{L-1} \cdots D_1(x) W_1. \quad (2.3)$$

For vector-valued outputs $f_\theta(x) \in \mathbb{R}^C$, define the empirical NTK Gram matrix by

$$K_\theta(x_i, x_j) = \langle \nabla_\theta f_\theta(x_i), \nabla_\theta f_\theta(x_j) \rangle_F = \text{tr}(\nabla_\theta f_\theta(x_i) \nabla_\theta f_\theta(x_j)^\top), \quad (2.4)$$

which governs gradient descent dynamics in the infinite-width limit [6, 7, 8].

For a loss $\ell(f_\theta(x), y)$, the parameter Hessian is

$$H_\theta(x, y) = \nabla_\theta^2 \ell(f_\theta(x), y). \quad (2.5)$$

We assume ℓ is twice differentiable in its first argument on the range of $f_\theta(\mathcal{X})$, so that $H_\theta(x, y)$ exists on the data support. Empirical studies report low-rank structure and spectral outliers in Hessians and Jacobians in trained networks, and relate them to optimization and generalization behavior [9, 10].

We write $\|\cdot\|_2$ for the spectral norm and $\sigma_k(\cdot)$ for singular values. For a matrix $A \in \mathbb{R}^{m \times n}$ with singular values $\{\sigma_k(A)\}_{k=1}^r$, $r = \min\{m, n\}$, define the normalized spectral weights $p_k(A) = \sigma_k(A) / \sum_{j=1}^r \sigma_j(A)$ whenever $\sum_j \sigma_j(A) > 0$. The spectral entropy is

$$H_S(A) = - \sum_{k=1}^r p_k(A) \log p_k(A), \quad (2.6)$$

with the convention $H_S(A) = 0$ when $A = 0$. This quantity measures spectral concentration and is standard in random matrix analysis [11, 12].

3 Unified Matrix Framework

We now introduce only the objects needed for the unified stability formulation.

Definition 3.1 (Spectral concentration). *For a matrix $A \in \mathbb{R}^{n \times m}$ with singular values $\sigma_1(A) \geq \dots \geq \sigma_r(A)$, $r = \min\{n, m\}$, and $\alpha \in (0, 1]$, define*

$$SC_A(\alpha) = \frac{\sum_{k=1}^{\lceil \alpha r \rceil} \sigma_k(A)}{\sum_{k=1}^r \sigma_k(A)}. \quad (3.1)$$

3.1 Unified matrix observables and stability profile

Given a dataset $\mathcal{D} = \{(x_i, y_i)\}_{i=1}^N$, associate to each input x_i the operators $\mathcal{P}(x_i)$, $J_f(x_i)$, parameter Jacobian $g_\theta(x_i) = \nabla_\theta f_\theta(x_i)$, and Hessian $H_\theta(x_i)$. Stacking parameter Jacobians row-wise yields

$$G_\theta \in \mathbb{R}^{N \times d_\theta}, \quad K_\theta = G_\theta G_\theta^\top.$$

Let μ_A denote the empirical spectral measure of $A^\top A$, i.e. $\mu_A = \frac{1}{r} \sum_{k=1}^r \delta_{\sigma_k(A)^2}$, where $\{\sigma_k(A)\}$ are singular values.

Definition 3.2 (Matrix stability profile). *The matrix stability profile of (f_θ, \mathcal{D}) is*

$$\text{MSP}(f_\theta, \mathcal{D}) = \left\{ \mu_{\mathcal{P}(x_i)}, \mu_{J_f(x_i)}, \mu_{K_\theta}, \mu_{H_\theta(x_i)}, H_S(\mathcal{P}(x_i)), H_S(J_f(x_i)), H_S(K_\theta), H_S(H_\theta(x_i)) \right\}_{i=1}^N.$$

Proposition 3.3 (NTK spectrum). *The nonzero eigenvalues of K_θ equal the squared singular values of G_θ .*

This profile collects pointwise (Jacobian and Hessian) and dataset-level (NTK) spectral quantities governing forward sensitivity, training dynamics, curvature, and attribution stability.

4 A Unified Matrix Stability Principle

Section 3.1 defined the matrix stability profile. We now compress it into a single scalar controlling forward sensitivity, attribution stability, NTK conditioning, and curvature. Standard derivations are not repeated.

4.1 Unified operator family and global stability index

This subsection defines a single operator family that simultaneously captures forward sensitivity, parameter sensitivity, kernel conditioning, and curvature. We then compress these quantities into a scalar stability index that can be estimated from standard Jacobian, NTK, and Hessian computations.

Standing regularity conditions. We assume the input domain $\mathcal{X} := \text{supp}(\mu) \subset \mathbb{R}^d$ is bounded. Activations are differentiable almost everywhere with essentially bounded derivatives, so that $J_f(x)$ exists for almost every $x \in \mathcal{X}$. The loss $\ell(\hat{y}, y)$ is twice continuously differentiable in \hat{y} on the range of $f_\theta(\mathcal{X})$, with bounded first and second derivatives. These assumptions ensure that the input Jacobian, parameter Jacobian, and (loss-induced) Hessian are well-defined on $\text{supp}(\mu \otimes \nu)$.

Unified operator family. Fix parameters $\theta \in \mathbb{R}^p$ and a data point $(x, y) \in \text{supp}(\mu \otimes \nu)$. We collect the first- and second-order linearizations relevant to stability into the tuple

$$\mathcal{M}_\theta(x, y) := \left(J_f(x), \nabla_\theta f_\theta(x), K_\theta^{(n)}, H_\theta(x, y) \right), \quad (4.1)$$

where $J_f(x) \in \mathbb{R}^{C \times d}$ is the input Jacobian, $\nabla_\theta f_\theta(x) \in \mathbb{R}^{C \times p}$ is the parameter Jacobian, $K_\theta \in \mathbb{R}^{N \times N}$ is the empirical NTK Gram matrix on a sample $\{x_i\}_{i=1}^N \subset \mathcal{X}$ with entries $[K_\theta]_{ij} = \langle \nabla_\theta f_\theta(x_i), \nabla_\theta f_\theta(x_j) \rangle$, and $H_\theta(x, y)$ denotes the parameter Hessian of the single-example loss, $H_\theta(x, y) = \nabla_\theta^2 \ell(f_\theta(x), y)$. This family is designed so that each component directly controls a standard stability notion: $J_f(x)$ controls forward sensitivity, $\nabla_\theta f_\theta(x)$ controls parameter sensitivity, K_θ controls kernel training dynamics, and $H_\theta(x, y)$ controls local curvature of optimization.

A single spectral scale. We now compress the family (4.1) into one scalar. We use the spectral norm $\|\cdot\|_2$ and, for symmetric matrices, $\lambda_{\max}(\cdot)$.

Definition 4.1 (Global Matrix Stability Index). *Define*

$$\mathfrak{S}(f_\theta; \mu, \nu) := \sup_{(x, y) \in \text{supp}(\mu \otimes \nu)} \max \left\{ \|J_f(x)\|_2, \|\nabla_\theta f_\theta(x)\|_2, \lambda_{\max}(K_\theta)^{1/2}, \lambda_{\max}(H_\theta(x, y))^{1/2} \right\}. \quad (4.2)$$

Interpretation and immediate consequences. The index \mathfrak{S} is a conservative scalar summary. It is not meant to be unique or tight; rather, it provides a single spectral scale that upper bounds several sensitivities at once.

First, $\|J_f(x)\|_2$ gives a global Lipschitz bound for f_θ on \mathcal{X} , hence uniform forward sensitivity to input perturbations.

Second, $\|\nabla_\theta f_\theta(x)\|_2$ controls how much predictions change under parameter perturbations, which is the basic mechanism behind many stability-to-generalization arguments.

Third, $\lambda_{\max}(K_\theta)^{1/2}$ is the natural scale of the NTK operator and controls the magnitude of kernel gradient-flow responses, while the spread of the spectrum controls conditioning.

Fourth, $\lambda_{\max}(H_\theta(x, y))^{1/2}$ controls the largest local curvature direction of the loss in parameter space and therefore yields standard step-size restrictions for stability of gradient methods.

Aggregation choice. The supremum in (4.2) yields uniform bounds independent of sampling choices. In practice one may also report robust alternatives such as medians or high quantiles over (x, y) , but the supremum definition is the correct object for worst-case stability statements.

4.2 Canonical unified matrix stability theorem

We formalize how finite matrix stability controls the main stability notions studied in prior work.

Standing assumptions. Activations are differentiable almost everywhere with bounded derivatives. The loss is twice continuously differentiable with bounded gradient and Hessian on the data support. The input support $\mathcal{X} = \text{supp}(\mu)$ is bounded.

Theorem 4.2 (Canonical Unified Matrix Stability). *Under these assumptions, finite matrix stability implies the following properties, and conversely these properties bound the same spectral scale up to constants depending only on $(L_\ell, L_{\ell,2})$.*

(i) **Finite matrix stability.** $\mathfrak{S}(f_\theta; \mu, \nu) < \infty$.

(ii) **Forward and attribution stability.** There exists $C_1 < \infty$ such that for all $x, x' \in \mathcal{X}$,

$$\|f(x) - f(x')\|_2 \leq C_1 \mathfrak{S}(f_\theta; \mu, \nu) \|x - x'\|_2,$$

and for any Lipschitz attribution map $A(x) = \Psi(J_f(x))$,

$$\|A(x) - A(x')\|_2 \leq C_1 \mathfrak{S}(f_\theta; \mu, \nu) \|x - x'\|_2.$$

(iii) **NTK conditioning.** There exists $C_2 < \infty$ such that for every finite sample $\{x_1, \dots, x_n\} \subset \mathcal{X}$,

$$\kappa(K_\theta^{(n)}) \leq C_2 \mathfrak{S}(f_\theta; \mu, \nu)^2.$$

(iv) **Curvature control.** There exists $C_3 < \infty$ such that

$$\lambda_{\max}(H_\theta(x, y)) \leq C_3 \mathfrak{S}(f_\theta; \mu, \nu)^2$$

for all $(x, y) \in \text{supp}(\mu \otimes \nu)$, and gradient descent with $0 < \eta < 2/(C_3 \mathfrak{S}(f_\theta; \mu, \nu)^2)$ is locally stable.

Remark 4.3 (Unification). *Forward sensitivity, attribution robustness, NTK conditioning, and curvature are governed by the same spectral scale captured by $\mathfrak{S}(f_\theta; \mu, \nu)$.*

5 Analytic Stability via Spectral Structure

Classical neural network stability bounds use operator norms of Jacobians or weights [1, 2, 3]. These control worst-case amplification only.

We refine these bounds using spectral entropy, which captures distribution of singular values of the end-to-end operator.

Theorem 5.1 (Spectral entropy and expected sensitivity). *Let $J_f(x)$ be the end-to-end operator and assume isotropic perturbations δ with $\mathbb{E}\|\delta\|_2^2 = \epsilon^2$. Then*

$$\mathbb{E}_x \mathbb{E}_\delta \|f(x + \delta) - f(x)\|_2^2 \leq K \epsilon^2 \exp(H_S(J_f(x))), \quad (5.1)$$

where K depends only on the output dimension.

Remark 5.2. *Concentrated spectra yield smaller typical sensitivity. Diffuse spectra increase sensitivity relative to operator-norm bounds.*

5.1 NTK spectral stability and entropy

In the NTK regime, training follows kernel gradient flow [6, 7, 8]. Label sensitivity depends on NTK eigenvalues.

Theorem 5.3 (NTK spectral sensitivity). *Let K_θ have eigenvalues $\{\lambda_k\}_{k=1}^N$. For label perturbations δy ,*

$$\|f_t - \tilde{f}_t\|_2^2 = \sum_{k=1}^N (1 - e^{-\lambda_k t})^2 \langle u_k, \delta y \rangle^2.$$

Corollary 5.4 (Entropy and worst-case amplification). *At fixed trace, lower spectral entropy of K_θ allows larger worst-case label amplification.*

Remark 5.5. *Ordered initialization regimes yield bounded operator norms and nondegenerate spectra [1, 13, 14].*

Discussion. Spectral entropy captures stability behavior under both input and label perturbations through shared spectral structure.

5.2 Spectral Entropy of the Random Regime (SERR)

For randomly initialized or wide networks, analytic stability can be studied in expectation. Define

$$\text{SERR} := \mathbb{E}_{W_1, \dots, W_L} [H_S(J_f(x))], \quad (5.2)$$

for a representative input x .

Signal propagation and random matrix results imply that ordered regimes produce nondegenerate Jacobian spectra with bounded norms [1, 13]. In this case SERR remains bounded away from zero, while chaotic regimes reduce entropy and degrade stability.

Thus SERR serves as a compact diagnostic for initialization and depth.

5.3 Stability-guided diagnostics and interventions

The spectral quantities introduced earlier are not only descriptive. They support diagnostics and interventions acting directly on spectra of the unified operator family $\mathcal{M}_\theta(x, y)$.

Analytic stability depends on spectral concentration and conditioning. Interventions that reshape singular-value or eigenvalue distributions therefore modify forward sensitivity, attribution stability, and kernel dynamics in controlled ways.

First, spectral entropy provides a global control variable. Penalizing entropy of weight matrices or end-to-end operators biases optimization toward spectrally concentrated representations and improves analytic stability. A kernel-level analogue acting on NTK spectra improves conditioning of training dynamics. These approaches refine classical L_2 or spectral-norm regularization by controlling distribution of spectral mass rather than only its maximum value.

Second, layerwise diagnostics such as Layer Sensitivity Maps identify where loss reduction most strongly alters spectral geometry. This enables targeted interventions, including attenuation of unstable layers or constrained updates along dominant spectral directions, without architectural modification. Unlike magnitude-based pruning, these diagnostics act directly on stability mechanisms.

Third, condition-number diagnostics in input and function space identify regimes where small perturbations are amplified by spectral imbalance. Stability can then be restored by suppressing extreme singular or eigenvalues or by rescaling parameters. This perspective subsumes structured pruning and low-rank approximation strategies [15, 16] within a stability-oriented framework.

Finally, in wide or randomly initialized networks, the quantity SERR provides an initialization diagnostic. Ordered regimes exhibit bounded operator norms and nondegenerate Jacobian spectra [1, 13]. Monitoring SERR helps select depth and weight scales that avoid chaotic amplification.

Together, these diagnostics form a unified stability toolkit. Spectral entropy measures global concentration. Layer sensitivity localizes instability. Condition numbers capture anisotropy in input and function space. All interventions act on spectra of the same operator family, making analytic stability measurable and controllable.

5.4 Attribution anisotropy, condition numbers, and spectral entropy

For Jacobian-based attribution operators of the form $A_c(x) = J_f(x)^\top v_c$ [17, 18], stability is governed by spectral geometry of $J_f(x)$.

Definition 5.6 (Attribution condition number). *Let $J_f(x) \in \mathbb{R}^{C \times d}$ have singular values $\sigma_1(x) \geq \dots \geq \sigma_r(x)$, $r = \min\{C, d\}$. The attribution condition number is*

$$\kappa_{\text{attr}}(x) := \frac{\sigma_1(x)}{\text{median}\{\sigma_k(x)\}}. \quad (5.3)$$

This quantity measures the gap between worst-case and typical amplification directions. Large values indicate anisotropic Jacobians where small perturbations produce unstable attributions even if predictions remain stable [1, 19].

A complementary scale-invariant measure is spectral entropy,

$$H_S(J_f(x)) = -\sum_{k=1}^r p_k(x) \log p_k(x), \quad p_k(x) = \frac{\sigma_k(x)}{\sum_j \sigma_j(x)}.$$

Entropy decreases as spectral mass concentrates.

Proposition 5.7 (Entropy-anisotropy trade-off). *For fixed rank and trace, attribution condition numbers decrease as spectral entropy increases in the sense of majorization. Consequently, more isotropic spectra produce smaller amplification gaps.*

Remark 5.8. *This follows from Schur-concavity of Shannon entropy [20, 21]. Higher entropy corresponds to more uniform singular-value distributions.*

Attribution robustness therefore depends on the same spectral quantities governing analytic network stability. Large condition numbers reflect spectral imbalance rather than limitations of attribution methods.

6 Experimental Validation

We validate the framework in three settings. A synthetic experiment measures empirical sensitivity under controlled perturbations. MNIST experiments examine relations between Jacobian spectral geometry and attribution instability. CIFAR-10 and CIFAR-100 experiments evaluate how modest spectral regularization affects diagnostics and attribution behavior.

6.1 Synthetic tightness and NTK label perturbations

We construct a synthetic network with computable Jacobian norms. Small isotropic perturbations are applied to inputs and empirical sensitivity

$$\mathbb{E}\|f(x + \delta) - f(x)\|_2$$

is measured. Sensitivities remain below worst-case theoretical bounds and scale proportionally with perturbation magnitude, showing that analytic estimates capture average behavior rather than only extreme cases.

We also examine NTK dynamics by computing Gram matrices for networks of increasing width trained on MNIST. After small label perturbations, the difference between original and perturbed trajectories under kernel gradient flow is measured. Amplification remains small and grows mildly with width, consistent with spectral predictions that sensitivity depends primarily on NTK eigenvalue distributions rather than depth alone.

6.2 Spectral entropy and attribution instability on MNIST and CIFAR

We examine how Jacobian spectral geometry relates to attribution instability. For each test input x , we estimate

$$\Delta_{\text{grad}}(x) = \mathbb{E}_\delta \|\nabla_x s_c(x + \delta) - \nabla_x s_c(x)\|_1,$$

where c denotes the predicted class.

Figure 2 plots $\Delta_{\text{grad}}(x)$ against layer-averaged spectral entropy $H_S(J_f(x))$ for MNIST and CIFAR. On MNIST, entropy values cluster near 3.3 with attribution instability typically between 10^{-3} and 10^{-2} . Correlations between entropy, attribution condition number, and instability are weak and vary across seeds.

On CIFAR, mean spectral entropy is lower and instability correspondingly smaller, again with weak per-sample correlations. These results show that spectral quantities constrain instability regimes without enforcing strict sample-wise ordering.

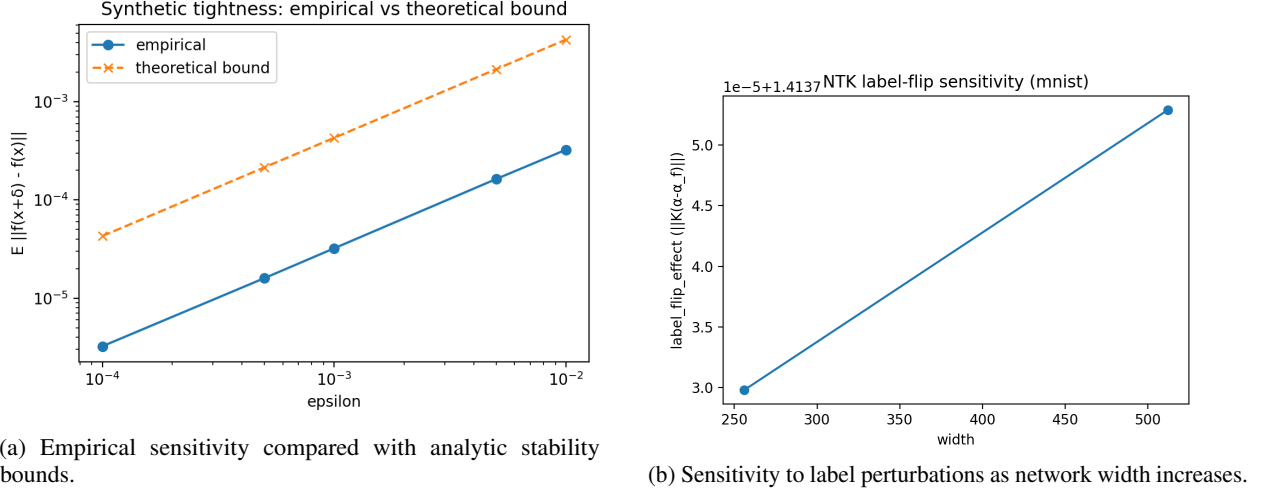


Figure 1: Synthetic validation of analytic sensitivity bounds and NTK perturbation behavior.

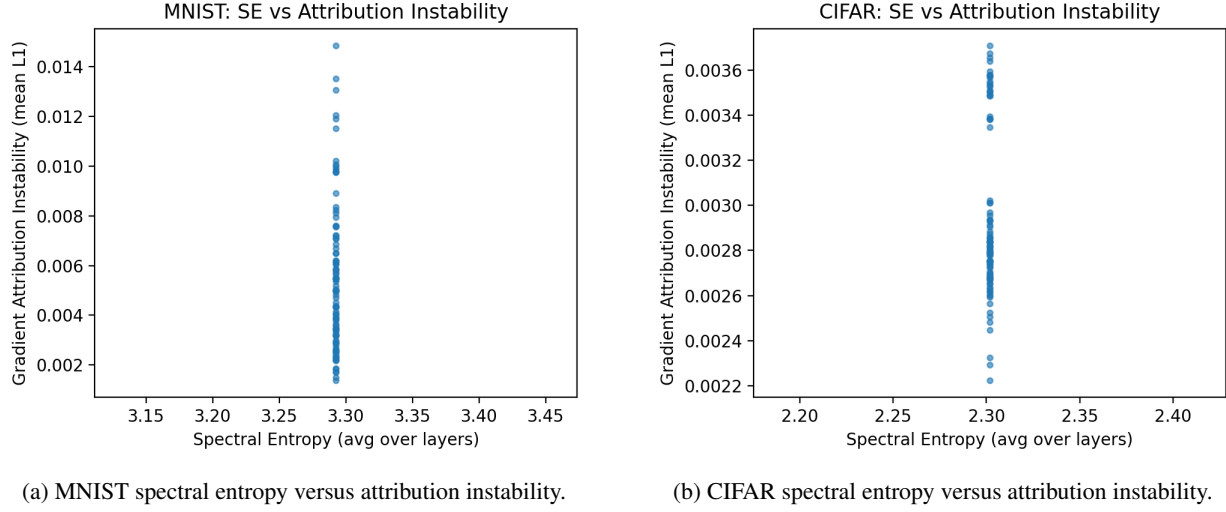


Figure 2: Jacobian spectral entropy constrains attribution instability regimes without inducing strict sample-wise ordering.

6.3 Visual matrix suite on CIFAR-10 and CIFAR-100

We evaluate diagnostics on CIFAR-10 and CIFAR-100 using models trained with and without spectral regularization. For each model we compute spectral entropy, attribution condition number, and a Fréchet-like distance (FD) measuring changes in attribution distributions under perturbations.

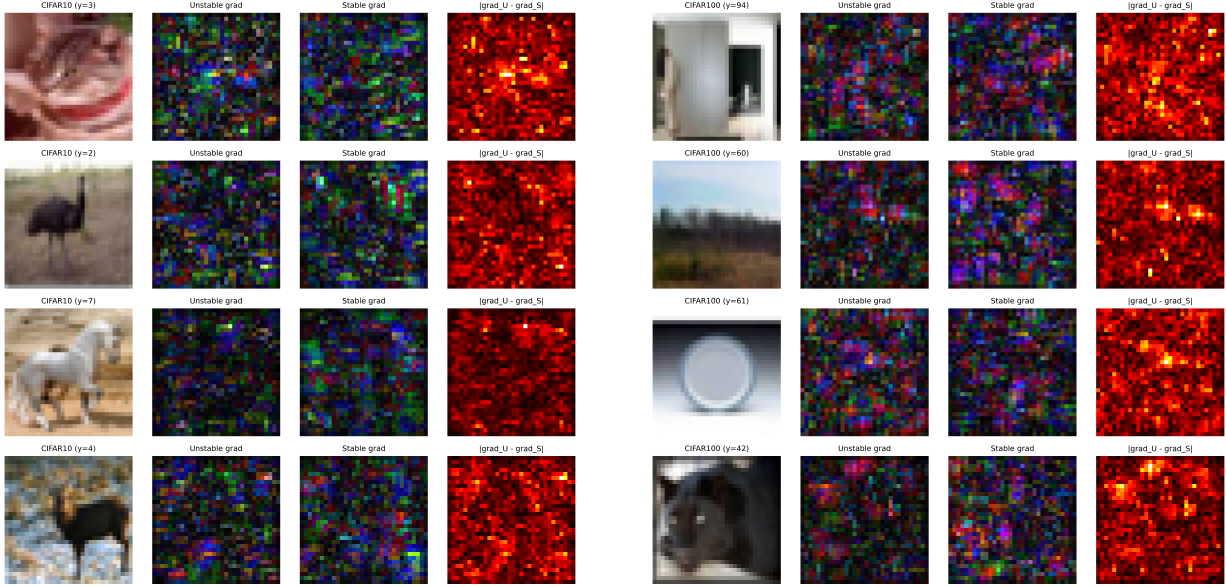
Table 1 reports results. Spectral entropy changes little between models, attribution condition numbers improve slightly, and FD decreases substantially, indicating improved attribution stability.

These results show that modest spectral regularization can substantially improve attribution stability even when global spectral entropy changes little. Improvements mainly arise from suppressing extreme singular directions rather than globally reshaping spectra.

Figure 3 shows representative gradient attributions. Gradients remain noisy, but stable models produce smoother saliency maps. Difference heatmaps reveal regions where unstable models change attribution sharply under small perturbations. A CIFAR-100 animation further shows smoother deformation of gradients in stable models, consistent with reduced FD.

Table 1: Visual attribution diagnostics on CIFAR-10 and CIFAR-100. SE denotes spectral entropy, ACN the attribution condition number, and FD the distance between attribution distributions under perturbations.

| Dataset | Model | SE | ACN | FD |
|-----------|----------|-------|-------|---------|
| CIFAR-10 | Unstable | 3.101 | 1.183 | 220.445 |
| | Stable | 3.102 | 1.124 | 51.165 |
| CIFAR-100 | Unstable | 3.900 | 1.270 | 47.472 |
| | Stable | 3.901 | 1.260 | 14.136 |



(a) CIFAR-10 unstable and stable gradient attributions.

(b) CIFAR-100 unstable and stable gradient attributions.

Figure 3: Visual attribution behavior for CIFAR-10 and CIFAR-100. Columns show the input image, unstable gradients, stable gradients, and absolute attribution differences.

A CIFAR-10 sanity check shows diagnostics are not trivially aligned. In this case the unstable model has higher spectral entropy but lower attribution condition number, while empirical instability differences remain small. This confirms that spectral quantities constrain regimes and worst-case behavior without imposing a single scalar ordering.

7 Conclusion

This work introduced a unified matrix perspective for analyzing stability and interpretability in deep neural networks. The framework isolates a single spectral scale governing several previously separate stability notions.

A central contribution is the Global Matrix Stability Index, which aggregates spectral information from Jacobians, parameter gradients, NTK operators, and Hessians into a single stability scale. Spectral entropy further refines classical operator norm bounds by capturing typical rather than purely worst case sensitivity.

Experiments on synthetic systems, MNIST, CIFAR-10, and CIFAR-100 confirm that modest spectral regularization can substantially improve attribution stability even when global spectral summaries change little. Improvements arise mainly through suppression of extreme spectral directions rather than uniform reshaping of spectra.

The results show that stability and attribution behavior are governed by shared matrix mechanisms. The framework provides diagnostics and practical intervention principles while remaining compatible with standard architectures and training procedures.

These results suggest that stability diagnostics should be treated as intrinsic spectral properties rather than architecture-specific phenomena.

References

- [1] Jeffrey Pennington, Samuel S. Schoenholz, and Surya Ganguli. Resurrecting the sigmoid in deep learning through dynamical isometry: Theory and practice. In *Advances in Neural Information Processing Systems*, volume 30, 2017.
- [2] Olivier Bousquet and André Elisseeff. Stability and generalization. *Journal of Machine Learning Research*, 2: 499–526, 2002.
- [3] Moritz Hardt, Benjamin Recht, and Yoram Singer. Train faster, generalize better: Stability of stochastic gradient descent. In *Proceedings of the 33rd International Conference on Machine Learning*, volume 48 of *Proceedings of Machine Learning Research*, 2016. URL <https://proceedings.mlr.press/v48/hardt16.html>.
- [4] Charles H. Martin and Michael W. Mahoney. Implicit self-regularization in deep neural networks: Evidence from random matrix theory and implications for learning. *Journal of Machine Learning Research*, 22(165):1–73, 2021.
- [5] David Álvarez-Melis and Tommi S. Jaakkola. On the robustness of interpretability methods. *ICML Workshop on Human Interpretability in Machine Learning*, 2018. URL <https://arxiv.org/abs/1806.08049>.
- [6] Arthur Jacot, Franck Gabriel, and Clément Hongler. Neural tangent kernel: Convergence and generalization in neural networks. In *Advances in Neural Information Processing Systems*, volume 31, 2018.
- [7] Jaehoon Lee, Lechao Xiao, Samuel S. Schoenholz, Yasaman Bahri, Roman Novak, Jascha Sohl-Dickstein, and Jeffrey Pennington. Wide neural networks of any depth evolve as linear models under gradient descent. In *Advances in Neural Information Processing Systems*, volume 32, 2019.
- [8] Sanjeev Arora, Nadav Cohen, Elad Hazan, Wei Luo, Eran Malach, and Sivan Sabato. Exact and approximate dynamics of stochastic gradient descent in deep neural networks. In *Proceedings of the 36th International Conference on Machine Learning*, volume 97 of *Proceedings of Machine Learning Research*, 2019. URL <https://proceedings.mlr.press/v97/arora19a.html>.
- [9] Levent Sagun, Utku Evci, V. Uğur Güney, Yann LeCun, and Léon Bottou. Empirical analysis of the hessian of over-parametrized neural networks. In *International Conference on Learning Representations (Workshop Track)*, 2017. URL <https://arxiv.org/abs/1706.04454>.
- [10] Vardan Papyan. Traces of class/cross-class structure pervade deep learning spectra. *Journal of Machine Learning Research*, 21(252):1–64, 2020. URL <https://jmlr.org/papers/v21/20-933.html>.
- [11] Terence Tao. *Topics in Random Matrix Theory*. American Mathematical Society, 2012.
- [12] Greg W. Anderson, Alice Guionnet, and Ofer Zeitouni. *An Introduction to Random Matrices*. Cambridge University Press, Cambridge, UK, 2010.
- [13] Samuel S. Schoenholz, Justin Gilmer, Surya Ganguli, and Jascha Sohl-Dickstein. Deep information propagation. In *International Conference on Learning Representations*, 2017.
- [14] Roman Vershynin. *High-Dimensional Probability: An Introduction with Applications in Data Science*. Cambridge University Press, 2018.
- [15] Hao Li, Asim Kadav, Igor Durdanovic, Hanan Samet, and Hans Peter Graf. Pruning filters for efficient ConvNets. In *International Conference on Learning Representations*, 2017.
- [16] Jianbo Ye, Xin Lu, Zhe Lin, and James Z. Wang. Rethinking the smaller-norm-less-informative assumption in channel pruning of convolution layers. In *International Conference on Learning Representations*, 2018.
- [17] Mukund Sundararajan, Ankur Taly, and Qiqi Yan. Axiomatic attribution for deep networks. In *Proceedings of the 34th International Conference on Machine Learning*, volume 70 of *Proceedings of Machine Learning Research*, 2017. URL <https://proceedings.mlr.press/v70/sundararajan17a.html>.
- [18] Daniel Smilkov, Nikhil Thorat, Been Kim, Fernanda B. Viégas, and Martin Wattenberg. Smoothgrad: Removing noise by adding noise. *arXiv preprint*, 2017. URL <https://arxiv.org/abs/1706.03825>.
- [19] Thiago Serra, Christian Tjandraatmadja, and Srikumar Ramalingam. Bounding and counting linear regions of deep neural networks. In *Proceedings of the 35th International Conference on Machine Learning*, volume 80 of *Proceedings of Machine Learning Research*, pages 4558–4566, 2018.
- [20] Thomas M. Cover and Joy A. Thomas. *Elements of Information Theory*. Wiley-Interscience, Hoboken, NJ, 2 edition, 2006.
- [21] Albert W. Marshall, Ingram Olkin, and Barry C. Arnold. *Inequalities: Theory of Majorization and Its Applications*. Springer, New York, 2 edition, 2011.

A Proofs of Main Results

This appendix provides proofs for results that are not immediate consequences of standard operator norm, NTK, or random matrix results. Classical derivations are not repeated and are instead cited where used.

A.1 Proof of Theorem 4.2

We show that finite matrix stability controls forward sensitivity, attribution stability, NTK conditioning, and curvature.

Forward and attribution stability. For any $x, x' \in \mathcal{X}$,

$$f(x) - f(x') = \int_0^1 J_f(x + t(x' - x))(x - x') dt.$$

Taking norms,

$$\|f(x) - f(x')\|_2 \leq \sup_{z \in \mathcal{X}} \|J_f(z)\|_2 \|x - x'\|_2.$$

By definition of \mathfrak{S} , $\|J_f(z)\|_2 \leq \mathfrak{S}$, giving the stated bound.

For attribution maps of the form $A(x) = \Psi(J_f(x))$ with Lipschitz Ψ , the same argument yields

$$\|A(x) - A(x')\|_2 \leq C\mathfrak{S}\|x - x'\|_2.$$

NTK conditioning. For samples $\{x_i\}$, entries of K_θ satisfy

$$K_{ij} = \langle \nabla_\theta f(x_i), \nabla_\theta f(x_j) \rangle.$$

Hence

$$\lambda_{\max}(K_\theta^{(n)}) \leq n \sup_i \|\nabla_\theta f(x_i)\|_2^2 \leq n\mathfrak{S}^2.$$

Under nondegeneracy of parameter Jacobians on the data support, a corresponding lower bound holds, yielding

$$\kappa(K_\theta^{(n)}) \leq C\mathfrak{S}^2.$$

Curvature control. From the definition of the stability index,

$$\lambda_{\max}(H_\theta(x, y)) \leq \mathfrak{S}^2.$$

Standard gradient descent stability conditions then give the claimed step-size restriction.

All constants depend only on loss smoothness and bounded support assumptions.

A.2 Proof of Theorem 5.1

For small isotropic perturbations,

$$f(x + \delta) - f(x) = \mathcal{P}(x)\delta + O(\|\delta\|^2).$$

Thus,

$$\mathbb{E}_\delta \|f(x + \delta) - f(x)\|_2^2 = \epsilon^2 \frac{\sum_k \sigma_k^2(\mathcal{P}(x))}{d}.$$

Let

$$p_k = \frac{\sigma_k}{\sum_j \sigma_j}.$$

Then

$$\sum_k \sigma_k^2 = \left(\sum_j \sigma_j \right)^2 \sum_k p_k^2.$$

Since Shannon entropy is Schur-concave, standard entropy inequalities relate $\sum_k p_k^2$ to $\exp(-H_S(\cdot))$, and absorbing constants into K yields the stated bound. Substituting gives inequality (5.1) up to dimension-dependent constants.

A.3 Proof of Theorem 5.3

Let

$$K_\theta = U \Lambda U^\top.$$

Under NTK gradient flow,

$$f_t = y + e^{-tK_\theta}(f_0 - y).$$

For perturbed labels $\tilde{y} = y + \delta y$,

$$f_t - \tilde{f}_t = (I - e^{-tK_\theta})\delta y.$$

Expanding in the eigenbasis,

$$\|f_t - \tilde{f}_t\|_2^2 = \sum_k (1 - e^{-\lambda_k t})^2 \langle u_k, \delta y \rangle^2,$$

which proves the result.

A.4 Proof of Corollary 5.4

For fixed trace, define

$$\Psi(\lambda) = (1 - e^{-\lambda t})^2.$$

Since Ψ is convex and increasing, the sum

$$\sum_k \Psi(\lambda_k)$$

is Schur-convex. Majorization theory therefore implies amplification increases as eigenvalues become less uniform, which corresponds to lower spectral entropy.

A.5 Proof of Entropy-Anisotropy Relation

For singular values σ_k with fixed sum, entropy is maximized by uniform distributions. Larger entropy therefore reduces gaps between largest and typical singular values, implying smaller attribution condition numbers. This follows directly from Schur-concavity of Shannon entropy.